INSTITUTE OF PHYSICS PUBLISHING SUPERCONDUCTOR SCIENCE AND TECHNOLOGY
Supercond. Sci. Technol. **19** (2006) 72–78 doi:10.1088/0953-2048/19/1/013

Transport AC losses of Ag-sheathed Bi-2223 tapes with different twist-pitch using electrical methods

M-H Jang[1] **and W Wong-Ng**[2]

[1] The Electrical and Computer Engineering Department, Yonsei University, 134 Shinchon-Dong Seodaemu-Gu, Seoul, Republic of Korea
[2] Ceramics Division, Materials Science and Engineering Laboratory, National Institute of Standards and Technology, Gaithersburg, MD 20899, USA

Received 9 September 2005, in final form 1 November 2005
Published 6 December 2005
Online at stacks.iop.org/SUST/19/72

Abstract
A series of Bi-2223 ([Bi, Pb]:Sr:Ca:Cu:O = 2:2:2:3) tapes with 37 superconducting core filaments was investigated in an attempt to correlate critical current and alternating current (AC) losses with twist-pitch. The twist-pitch of these multi-filamentary tapes which were produced by the powder-in-(Ag)tube (PIT) method varies from 8, 10, 13, 30, 50, 70 mm to ∞ mm (non-twist). Critical current (I_c) measurements which were conducted in zero field by a four-probe method under liquid-nitrogen temperature showed that I_c is greater in the non-twist filament than that in twisted filaments. Among these tapes, three (twist-pitch of 10, 13, and 70 mm) were selected for AC loss experiments under a time-varying transport current. The results of AC loss measurements in general agree with that of the AC loss simulation using the ellipse model of the Norris equation. Simulation results show that the hysteretic AC loss is lowest in the non-twist tape and increases as the twist-pitch decreases. A much greater loss was found in tapes with small twist-pitch, i.e. 10 and 8 mm. Among different possible loss contributions to the total AC losses, the hysteretic loss was determined to be the main source. In addition, microstructural damage of tapes with small twist-pitch appears to contribute to the overall AC losses as well.

(Some figures in this article are in colour only in the electronic version)

1. Introduction

Recent achievements in the fabrication of long-length multi-filament [Bi, Pb]–Sr–Ca–Cu–O (BSCCO) high-temperature superconductor (HTS, Type II) tapes with high critical current have generated considerable interest for applications such as cables, transformers, motors, generators, and energy storage systems. At present, BSCCO-based tapes are the only high-T_c superconductors that have a commercial market. Improvement of processing of these tapes, however, is still needed in order to maximize the superconducting properties which in turn will lead to the minimization of cost of production. Since BSCCO tapes in most large-scale systems are exposed to time-varying fields (transport alternating current (AC)), these tapes exhibit energy dissipation mainly due to AC losses. Much research has been directed towards understanding of the nature and minimization of these AC losses [1–27].

The AC losses of a superconductor tape are dependent on the geometry of the filaments in the tape, the magnetic and electrical properties of the superconductor, the type of matrix materials, and the amplitude and frequency of the transport current. The total AC losses, Q, are attributed to hysteretic loss within the filaments (Q_h), eddy current loss and coupling current loss within the matrix (Q_e), and coupling current loss across the matrix (Q_c). The total energy dissipation due to the AC losses is determined by a complicated interaction between these individual loss components. The critical state model has been used extensively to describe the electrodynamics of type II superconductors and to calculate the AC hysteresis losses [28, 29]. For Bi-2223 ([Bi, Pb]:Sr:Ca:Cu:O = 2:2:2:3)-

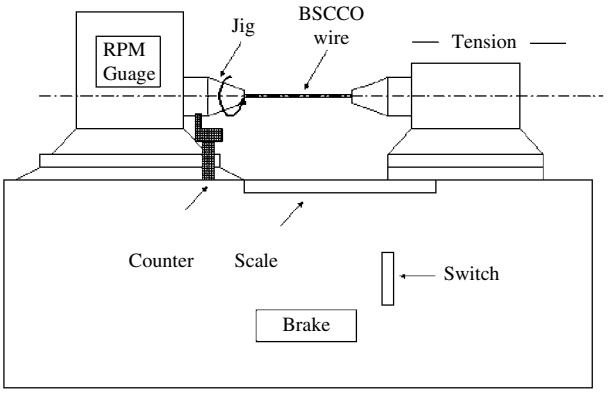

Figure 1. Schematic drawing of the experimental apparatus used for twisting the multi-filamentary Bi-2223/Ag tapes.

based tapes consisting of multiple superconducting cores in a silver matrix, the AC losses were found to be mostly frequency independent [28–30]. Among the loss components in the BSCCO tapes, the hysteretic loss and coupling current loss appear to be the dominant factors. It was reported by Eckelmann *et al* that, by twisting the filaments before rolling into a flat tape, one can reduce the coupling current loss [31]. It is also known that filament twisting can reduce AC losses in the transverse magnetic field [31–42]. AC losses in filamental BSCCO tapes, in general, can be effectively reduced when the filament size, the electrical resistivity of the matrix, and the twist-pitch of the filaments are properly modified [36].

In this paper, we report the results of critical current measurements and AC loss simulation of a series of BSCCO tapes using the Norris equation with different twist-pitch (8, 10, 13, 30, 50, 70 mm and ∞). Experimental AC loss measurements were further performed on three selected tapes with twist pitch of 10, 13, and 70 mm. In summary, critical currents of these BSCCO tapes were measured by controlling the applied transport current (at a fixed 60 Hz) to be perpendicular to the *c*-axis of the tape. The transport current method was used by Majoros *et al* [17] to measure the AC losses by varying the transport alternating current (1–12 A) and the incident angle between the *c*-axis of the tape and the electrical field. Experimental AC losses of our samples were compared with simulated data obtained by the Norris equation using the ellipse model (discussed below). The influence of the interior structure (i.e. different twist-pitch and microstructure) on the transport current and AC losses was evaluated.

2. Experimental details[3]

2.1. Manufacturing of multi-filament silver-sheathed Bi-2223/Ag tapes

Multi-filament silver-sheathed $Bi_{1.8}Pb_{0.4}Sr_{2.0}Ca_{2.2}Cu_{3.0}O_{10+x}$ (Bi-2223/Ag matrix) tapes were prepared by a powder-in-tube (PIT) technique where a high *c*-axis grain alignment was achieved by a combination of repeated rolling, pressing, and heating [43]. To prepare the Bi-2223 powder, appropriate amounts of Bi_2O_3, $SrCO_3$, $CaCO_3$ and CuO were mixed and milled for 24 h in methanol with ZrO_2 media. The milled slurry was dried and then calcined at 700 °C for 12 h, 800 °C for 8 h, 835 °C for 8 h, and 855 °C for 8 h. The calcination and grinding procedure was repeated three times.

To prepare the Ag-sheathed filament wire, the Bi-2223 powder was loaded into silver tubing (6.35 mm outer diameter, 4.35 mm inner diameter), followed by repeated swagings and drawings through a series of dies to a final diameter of 1.75 mm. Each drawing step reduced the diameter of the monofilament wire by less than 10%. To relieve the stress of the cold-worked Ag sheath, intermediate annealings were incorporated between successive swagings and drawings.

Multi-filament BSCCO conductors were fabricated by rearranging 37 monofilament wires in a Ag tubing with an outer diameter of 14 mm and an inner diameter of 12 mm. The tubes were drawn to a final diameter of 1.54 mm with a drawing procedure similar to that used for the monofilament conductors. The conductors were then cut into 30 cm long segments, and twisted to various twist-pitches by turning each end with a specially designed twisting machine. Figure 1 shows a schematic diagram of the apparatus used for twisting these Bi-2223/Ag tapes. In the twisting process, a predetermined number of turns were applied to the wires in order to produce the desired twist-pitch (8, 10, 13, 30, 50, 70 mm and ∞ (non-twist); designated as tape I, II, III, IV, V, VI and VII, respectively) after rolling to the final thickness of tape. The speed of drawing (RPM) was usually between 32 and 2000 RPM depending on the length of the twist-pitch. During twisting, the sample was annealed at 400 °C for 30 min in order to minimize microstructural damage. After the twisting process, the tapes were further rolled and annealed at 840 °C for 50 h. These tapes have a nominal thickness of about 0.25 mm.

The microstructural study which was critical to evaluate the uniformity of the superconductor filaments that were deformed during the twisting process was reported previously [44]. In brief, the microstructure of these tapes was investigated by optical and scanning electron microscopy (SEM) on both the polished and fractured surfaces. The degree of texturing, the twist-pitch, and the presence of cracks were determined after etching the Ag sheath with a mixture of H_2O_2:NH_3 = 1:1 [45].

2.2. Critical current and electrical losses (power consumption) measurements

The critical current (I_c) of samples with different twist-pitch were measured at 77 K by a standard four-probe technique. The measurements were performed in a zero-applied magnetic field (a 1 μV cm^{-1} applied voltage) by an applied transport current with a frequency of 60 Hz.

Figure 2 shows the schematic drawing of the experimental apparatus for electrical AC loss measurement with the electrical method. According to Kang *et al* [46], when an AC current transports in a superconductor tape, a magnetic flux is induced in the voltage lead (Ampere's law), and a voltage is also induced in the voltage lead (Maxwell's law):

$$V = \mathrm{d}/\mathrm{d}t \int (\mu_0 H + \mu_0 M)\,\mathrm{d}S, \qquad (1)$$

[3] Certain commercial equipment, instruments, or materials are identified in this paper in order to specify the experimental procedure adequately. Such identification is not intended to imply recommendation or endorsement by the Air Force Research Laboratory or the National Institute of Standards and Technology, nor is it intended to imply that the materials or equipment identified are necessarily the best available for the purpose.

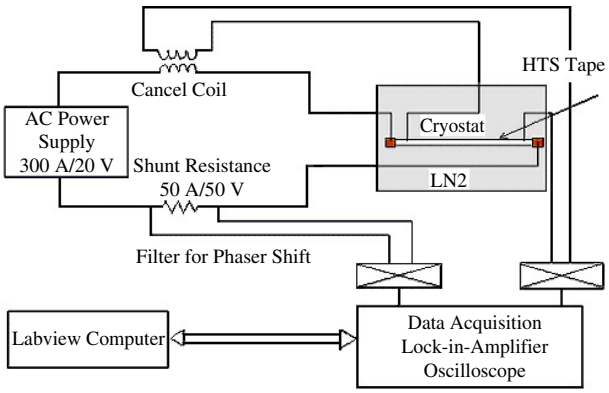

Figure 2. Schematic drawing of the experimental apparatus for AC loss measurement using the electrical method.

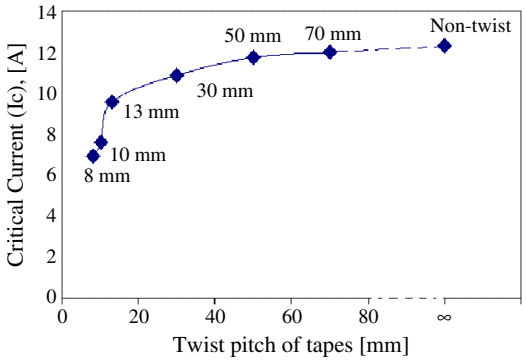

Figure 3. Variation of critical current of the Bi-2223/Ag tapes with twist-pitch (at 77 K).

where V is the induced voltage. The first integral term represents the inductive component and the second one is the resistive component of the induced voltage. Since the inductive component is not related to the AC loss, it must be cancelled by the cancel coil (figure 2). Therefore the electrical AC loss can be calculated by measuring $\mu_0 M$, the resistive signal. The measured induced voltage (V) is the sum of an AC loss component and an inductive component as shown in equation (1). The AC power loss is obtained by multiplying the loss component of the voltage with half the AC current amplitude. For current less than the tape's critical current I_c, the inductive component is much greater than the loss component. Therefore, to determine the loss component it is important to accurately determine the phase of the current through the tape.

For details of AC loss measurements, readers are referred to [47] and [48]. As shown in figure 2, the electrical AC loss measurements were carried out using a lock-in amplifier [7] which is part of the AC power supply, and a nanovoltmeter [33]. The lock-in amplifier is used to measure the in-phase and the quadrant components of the voltage of the tape where the reference signal is taken from the reference output of the sine generator [48]. The lock-in amplifier separates the cable voltage drop into in-phase and out-of-phase components with respect to the current flowing in the conductor. A reference signal with known phase with respect to the current phase is therefore necessary.

We have developed a perfectly inductive, Rogowsky-like cancel coil to provide a signal proportional to the current, but with a phase shift of 90°. The signal, which is in the conductor (and the coil) and is adjustable over a large range of amplitudes for compensating for the inductive component of the AC voltage, far exceeds the resistive one. In order to reach the maximum possible current amplitude in this system in spite of the presence of an inductive component far exceeding the resistive one, it is necessary for the amplifier output to contain resonant circuits. This arrangement will also improve the quality of the signal at a selected frequency.

A second lock-in-amplifier (oscilloscope) was used to measure the voltage drop produced in a perfectly resistive shunt by the output current of a current transformer of known radio frequency. All signals from the lock-in amplifier and the data acquisition device were stored in an analogue recorder.

Since the AC losses of the BSCCO tapes depend on the magnitude of the current, and do not depend on frequency under the present range of critical current, our studies were carried out under a variable transport current at a fixed frequency of 60 Hz. The three tapes that were selected for the AC loss experiments were tape II (twist-pitch of 10 mm), tape III (13 mm), and tape VI (70 mm).

3. Simulation studies of AC losses

The relation between AC *coupling current loss* (Q_c) and twist-pitch can be expressed by the following equations that were derived by Norris [30]:

$$Q_c = \frac{n\pi B_a^2 \omega \tau}{\mu_0(1+\omega^2\tau^2)} \tag{2}$$

and

$$\tau = \mu_0 \sigma_c L_p^2 \frac{d_c^2}{16\omega_c^2} \tag{3}$$

where Q_c is the coupling current loss, n is the sharp factor, B_a is the external field amplitude, ω is the angular frequency of the field, τ is a time constant, μ_0 is the initial permeability, σ_c is the conductivity of the matrix, L_p is the twist-pitch, and d_c and ω_c are the thickness and width of the tape core, respectively.

Based on the critical state model assuming constant critical current density, the magnetic field generated by a tape conductor can be approximated by an ellipse (4) or by a thin strip. It has been reported that in general the ellipse model is superior to the thin strip model in describing the AC loss of a tape [49, 50]. The *hysteretic current loss* (Q_h) of an HTS tape can be described by the ellipse model formulated by Norris:

$$Q_h = \frac{\mu_0 I_c^2}{\pi}[(2-\beta)\beta/2 + (1-\beta)\ln(1-\beta)] \tag{4}$$

where $\beta = I_0/I_c$, I_0 is the peak current, I_c is the critical current, and μ is the magnetic permittivity of free space ($4\pi \times 10^{-7}$ H m^{-1}). In this model the *hysteretic loss* does not depend on the dimensions of the tape. It is also noted that if the loss is normalized to the square of the critical current, then P/I_c^2 is a function of β only. Thus, plotting normalized loss versus I_0/I_c is a convenient way to compare the AC loss of these tapes with different I_c. The region with $\beta < 1.0$

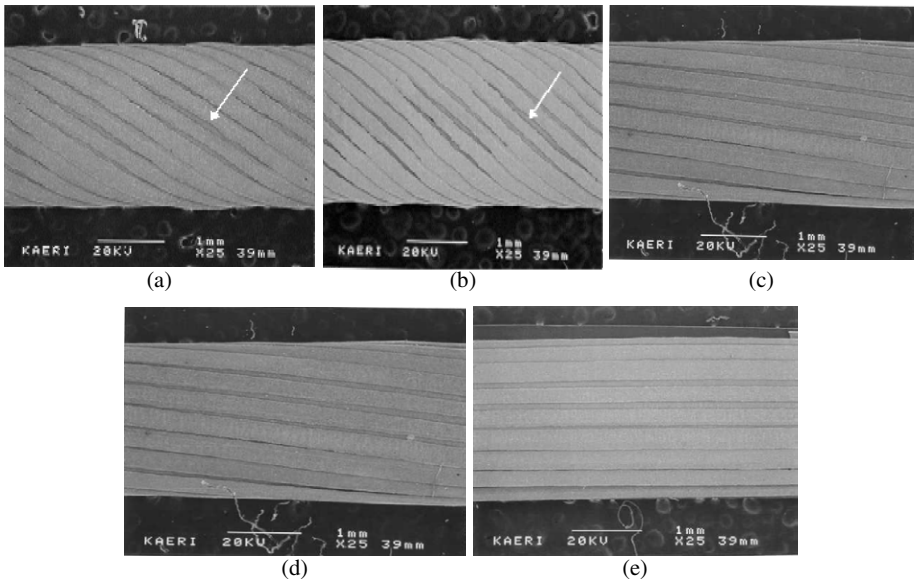

Figure 4. SEM images of BSCCO tapes with various twist-pitch: (a) tape II (10 mm), (b) tape III (13 mm), (c) tape IV (30 mm), (d) tape VI (70 mm), and (e) tape VII (non-twisted). Arrows indicate interface irregularity.

(where $\beta = I_0/I_c$) represents a hysteretic loss region. In this paper, we perform a simulation of the AC hysteretic losses of the twisted tapes using equation (4).

4. Results and discussion

4.1. Critical current

Figure 3 shows the twist-pitch dependence of critical current of the BSCCO tapes. The critical currents were measured to be 6.92, 7.6, 9.60, 10.87, 11.76, 12.01 and 12.34 A for tapes I, II, III, IV, V, VI, and VII, respectively. It is noted that the tapes with a low twist-pitch have relatively lower critical current. It was found that the critical current of these tapes decreases monotonically to 9.60 A when the twist-pitch is reduced from ∞ to 13 mm. It then decreases considerably faster and reaches a much smaller value of 6.92 A when the twist-pitch is reduced further to 8 mm. Only 52% of the critical current was retained for the 8 mm twisted-tape, as compared to the non-twisted tape.

Figures 4(a)–(e) show the SEM microstructure of the exposed filaments for tapes II, III, IV, VI and VII after etching of the Ag sheath [44]. The twist-pitches of the these tapes were measured to be 9.7, 12.5, 28.1 and 68.1 mm, respectively, which are nominally the same values as what we intended to prepare. From figure 4(e), it is noted that the filaments were almost uniformly deformed for the non-twist tape. However, the filaments in the twisted tapes were slightly degraded, particularly for tapes with small twist-pitch, as shown in figures 4(a) and (b). The slight degradation of tapes can reduce the critical current and mechanical strength of the tape. The interface irregularity can reduce the cross section of the superconducting cores and thus reduce the critical current.

The effect of twisting on the microstructural evolution such as grain size, grain alignment, and interface morphology on resulting critical current was discussed by Lim *et al* [44]. It was observed that grain size and the degree of texture of the BSCCO tapes decreased with decreasing pitch, probably due to the formation of the irregular interface between Ag and the filaments. The reduction of critical current may be related to the interface irregularity, smaller grain size, poorer texture and the presence of cracks due to the induced strain during the twisting process. The application of strain during the twisting process apparently causes irregular deformation to the microstructure of both the matrix and the superconducting core filaments, which may lead to local reduction of filament area, and reduce the critical current of the tape.

Several groups also reported that the grain size of the BSCCO phase was larger and the alignment was better near the interface between the Ag and the core than in the centre [51]. This observation suggested that the interface plays an important role in microstructural evolution. It was also suggested that the interface acts as a template for grain growth and alignment. For tapes with large twist-pitch, the larger grain size and better grain alignment are partly related to a straighter and more uniform interface.

4.2. AC losses

Table 1 summarizes the AC loss simulation result of tapes II, III and VI using the ellipse model of the Norris formula [30]. Figure 5 shows the simulated self-field hysteretic AC losses of the three twisted Bi-2223 tapes at 77 K as a function of the normalized current, I_0/I_c (ratio of the transport current to critical current; with $I_c = 7.6, 9.6$, and 12.01 A), for tape II, III and VI, respectively. Each curve in figure 4 ends at a different value because they are normalized with a different critical current limit beyond which the superconductor becomes normal. From figure 5, an AC loss value of 6.01, 4.02, and 3.04 μJ/m/cycle at $I_0/I_c = 0.6$, and 1.28, 0.92 and 0.81 μJ/m/cycle at $I_0/I_c = 0.4$ were obtained. We found that tape II, which has the smallest twist-pitch among the three tapes, has the greatest loss factor among the three tapes.

Figure 6 shows the measured total voltage (right-hand axis) and AC current (left-hand axis) of tape VI as a function

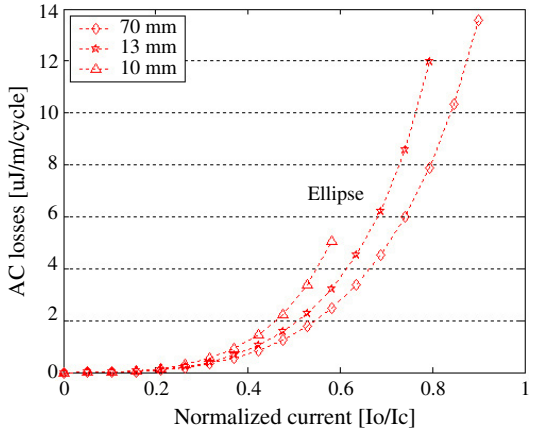

Figure 5. Simulated AC losses as a function of the normalized current (ratio of transport current to critical current [I_0/I_c]) in twisted multi-filamentary Bi-2223 tapes (tape II (twist-pitch of 10 mm), tape III (13 mm) and tape VI (70 mm)) using the Norris formula (ellipse model).

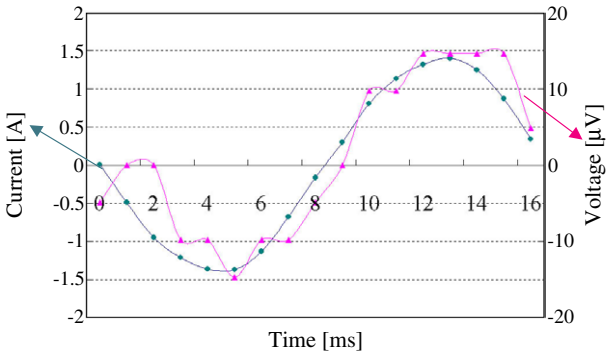

Figure 6. Wave-form of AC voltage and current (tape VI (twist-pitch of 70 mm)) as a function of time obtained by the electric method (at 77 K).

Table 1. AC losses of the three multi-filamentary Bi-2223/Ag tapes (37-core) by the Norris formula (ellipse model) and the electrical method at 77 K.

	AC losses (μJ/m/cycle)			
	Ellipse model		Experiment	
Sample	$I_0/I_c = 0.4$	$I_0/I_c = 0.6$	$I_0 = 6$ A	$I_0 = 8$ A
Tape I	0.81	3.04	1.3	2.8
Tape II	0.93	4.02	1.3	3.3
Tape III	1.29	6.01	1.7	3.8

of time during an AC cycle where $I_0/I_c = 1$ (right-hand axis). The rounded-shape curve displays the AC current, I. The fluctuated voltage $V(t)$, which is related to the total electrical AC losses, becomes large when a large portion of the current is forced to flow through the silver sheath. The experimental curve describes accurately the self-field AC power loss, P_L (where $P_L = P_{\text{real}}/(\omega I_c^2)$, ω is the angular frequency of the field), indicating that the experimental AC loss data measured at 60 Hz are real and reliable.

Figure 7 shows the experimental transport AC losses (1–12 A) for tape II, tape III, and tape VI by using the

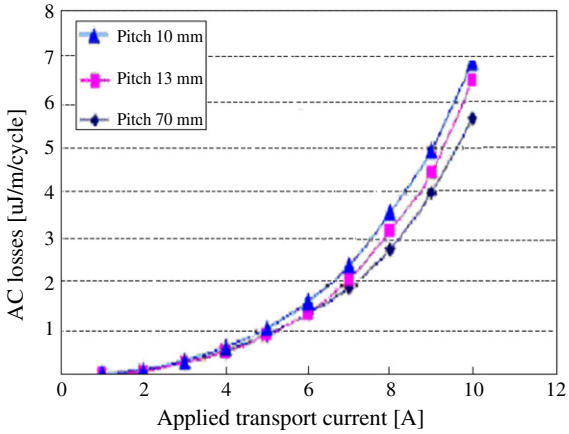

Figure 7. Experimental AC losses as a function of applied transport alternating current (1–12 A) in twisted multi-filamentary Bi-2223 tapes (tapes II, III and VI) by applying the electric method (at 77 K).

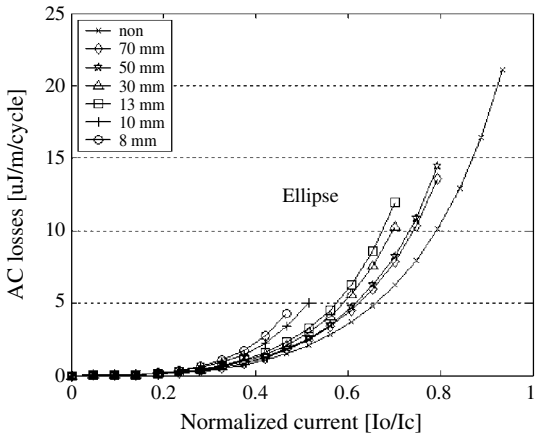

Figure 8. Simulated AC losses of the twisted multi-filamentary Bi-2223 tapes as a function of the ratio of transport current to critical current [I_0/I_c] calculated with the Norris formula (ellipse model) [30].

electrical method. From these experiments, it can be seen that the AC losses were generated almost as a curved quadratic curve dependent on transport current. The shape of these curves appears to agree with the simulated curves using the ellipse model (figure 5). It is also noted that the AC current losses of these tapes increased with decreasing twist pitch (table 1), and also increased considerably when a transport current greater than 3 A was applied. For example, the three tapes were found to have the same AC loss value of 0.4 μJ/m/cycle when the transport current is at a small value of 3 A. When a larger transport current, $I_0 = 6$ A, was applied, the corresponding AC loss values for these tapes increase to 1.7, 1.3 and 1.3 μJ/m/cycle, respectively. At $I_0 = 8$ A, the corresponding values are 3.8, 3.3 and 2.8 μJ/m/cycle. The AC losses of these tapes increase about 10, 8 and 7 fold for tape II, tape III and tape VI, respectively, when the applied current is increased from 3 to 8 A.

We have also simulated the AC loss curves of the entire seven multi-filamentary Bi-2223 tapes (tape I to tape VII), for which the critical current has been measured using the ellipse model of the Norris formula (figure 8)). This series

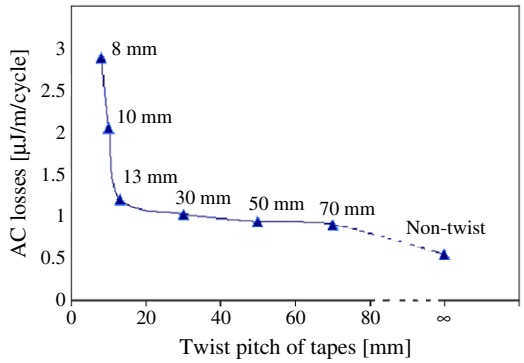

Figure 9. Variation of AC losses of the multi-filament BSCCO tapes with twist-pitch (at 77 K).

of curves clearly establishes a trend that the smaller the twist pitch of the tape, at a fixed transport current, the higher the magnitude of AC losses. In figure 9, we have plotted the maximum AC loss values of these tapes versus twist-pitch. It is noted that the shape of the curve of the maximum AC losses versus twist-pitch is related to the plot of critical current versus twist-pitch (figure 4). There is a steep increase of the AC losses as the twist-pitch decreases beyond 13 mm, mirroring the steep decrease of the critical current as shown in figure 4. Apparently there are common factors that are influencing the critical currents and AC losses.

From the previous discussion, the hysteretic AC loss obtained by using the ellipse model of the Norris equation increases as the twist-pitch decreases. From equations (2) and (3), although one expects that the coupling AC loss will increase as the twist-pitch decreases, it is by a much small quantity because the B_a value in equation (2) is small due to the fact that there is no external applied magnetic field. The microstructural changes (Ag matrix hardening by deformation, decrease in grain size, grain connectivity and in grain alignment in the filaments [44]) in the filaments as the twist-pitch decreases will likely contribute to the degradation of mechanical integrity and electrical property of the BSCCO tapes, resulting in an increase in AC losses.

5. Conclusion

The trend of critical current versus twist-pitch of a series of Bi-2223 tapes with different twist-pitch appears to be related to the shape of the curve of the maximum AC losses. In general, tapes with smaller twist-pitch have microstructural damage which in turn gives rise to low critical current and high AC loss.

The shapes and trends of the simulated hysteretic loss curves agree well with the observed experimental AC transport current loss curves. While the Norris equations suggest that both the coupling AC loss and the hysteretic AC loss (ellipse model) are higher in the BSCCO tapes with smaller twist-pitch, the coupling loss is a much smaller quantity for these tapes because of the absence of the external applied magnetic field.

In conclusion, we determined from this study that the two most important factors contributing to the observed trend of AC losses of the BSCCO tapes as a function of the twist-pitch are hysteretic loss and microstructural damage.

Acknowledgments

This work was supported by the Korean Research Foundation Grant (KRF-2004-050-D0003). The authors are also grateful for valuable discussions with Dr T K Ko and Dr J H Lim.

References

[1] Yoo J, Ko J, Kim H and Chung H 1999 *IEEE Trans. Appl. Supercond.* **9** 2163–6
[2] Yang Y, Hughes T J, Beduz C and Durmann F 1998 *Physica* C **310** 147–53
[3] Darmann F, Zhao R, Mccaughey G, Apperley M, Beals T P and Friend C 1999 *IEEE Trans. Appl. Supercond.* **9** 789–92
[4] Goldacker W, Eckelmann H, Quilitz M and Ullmann B 1997 *IEEE Trans. Appl. Supercond.* **7** 1670–3
[5] Cave J R, Fevrier A, Verhaege T, Lacaze A and Laumond Y 1991 *IEEE Trans. Magn.* **27** 2206–9
[6] Omen M P, Rieger J, Leghissa M, Fisher B and Arndt T 1997 *Physica* C **290** 281–90
[7] Omen M P, Rieger J, Leghissa M, Fisher B and Arndt Th 1998 *Physica* C **310** 137–41
[8] Fukunaga T, ltou T, Oota A, Maeda J and Hiroaoka M 1997 *IEEE Trans. Appl. Supercond.* **7** 1666–9
[9] Kunzler J E 1961 *Rev. Mod. Phys.* **33** 501
[10] Amemiya N, Jin F, Jiang Z, Shirai S, Haken B T, Rabbers J-J, Ayai N and Hayashi K 2003 *Supercond. Sci. Technol.* **16** 314–21
[11] Inada R, Ogawa Y, Inagaki N, Nakamura Y, Oota A and Zhang P X 2003 *Physica* C **392–396** 1091–5
[12] Martínez E, Hughes T J, Díez C, Angurel L A, Yang Y and Beduz C 1998 *Physica* C **310** 71–5
[13] Chen D-X, Luo X-M, Fang J-G and Han Z-H 2003 *Physica* C **391** 75–8
[14] Däumling M 1998 *Physica* C **310** 12–5
[15] Carr W J Jr 1998 *Physica* C **310** 1–5
[16] Boggs S A, Collings E W and Parish M V 1992 *IEEE Trans. Appl. Supercond.* **2** 117–21
[17] Majoros M, Jansak L, Zannella S, Curcio F, La Cascia P, Ottoboni V, Friend C M, Le Lay L, Glowacki B A and Campbell A M 1998 *Physica* C **310** 6–11
[18] Jang M H, Chu Y, Ko T K, Oh S S and Joo J H 2000 *Physica* C **341–348** 2575–6
[19] Fang J *et al* 2004 *Supercond. Sci. Technol.* **17** 1173–9
[20] Amemiya N, Miyamoto K, Murasawa S, Mukai H and Ohmatsu K 1998 *Physica* C **310** 30–5
[21] Amemiya N, Murasawa S, Murasawa S, Banno N and Miyamoto K 1998 *Physica* C **310** 16–29
[22] Takács S 2000 *Inst. Phys. Conf. Ser.* **167** 851–64
[23] Takács S, Iwakuma M and Funaki K 2001 *Physica* C **354** 265
[24] Eckelmann H, Däumling M, Quilitz M and Goldacker W 1998 *Physica* C **295** 198
[25] Däumling M 1998 *Supercond. Sci. Technol.* **11** 590
[26] Takács S 2005 *Supercond. Sci. Technol.* **18** 187–92
[27] Takács S and Gömöry F 2005 *Supercond. Sci. Technol.* **18** 340–5
[28] Polak M, Hlasnik I, Fukui S, Ikeda N and Tsukamoto O 1994 *Cryogenics* **34** 315–24
[29] Swan W 1968 *J. Math. Phys.* **9** 1308
[30] Norris W T 1970 *J. Phys. D: Appl. Phys.* **3** 489
[31] Eckelmann H, Quilitz M, Oomen M, Leghissa M and Goldacker W 1998 *Physica* C **310** 122–6
[32] Dhalle M, Polcari A, Marti F, Witz G, Huang Y B, Flukiger R, Clerc St and Kwasnitza K 1998 *Physica* C **310** 127–31
[33] Yang Y, Hughes T J, Beduz C and Darmann F 1998 *Physica* C **310** 147–53
[34] Iwakuma M, Tajika Y, Kajiwa K, Matsushita T, Otabe E S, Ayai N and Hayshi K 1998 *Physica* C **310** 154–8
[35] Staines M, Rupp S, Pooke D, Flesher S, DeMoranville K and Christopherson C 1998 *Physica* C **310** 163–7

[36] Gomory F and Christopherson C 1998 *Physica* C **310** 168–72
[37] Friend C M, Beduz C, Dutoit B, Navarro R, Cereda E and Alonso-Llorente J F 1999 *IEEE Trans. Appl. Supercond.* **9** 1165–8
[38] Hung Y B, Dhalle M, Marti F, Witz G and Flukiger R 1990 *IEEE Trans. Appl. Supercond.* **9** 1173–6
[39] Yang Y, Hughes T J, Martinerz E, Beduz C and Darmann F 1999 *IEEE Trans. Appl. Supercond.* **9** 1173–80
[40] Rabbers J J, van der Lann D C, ten Haken B and ten Kate H H J 1999 *IEEE Trans. Appl. Supercond.* **9** 1185–8
[41] Amemiya N 2000 *Adv. Cryog. Eng. (Mater.)* **46** 631–8
[42] Wilson M 1983 *Superconducting Magnets* (Oxford: Clarendon) p 174
[43] Brandt E H and Indenbom M 1993 *Phys. Rev.* B **48** 12893–906
[44] Lim J H, Joo J, Kim J G, Nah W, Jang M H, Ko T, Lee S J, Ha H S, Oh S S and Kwon Y K 2001 *IEEE Trans. Appl. Supercond.* **11** 2796–9
[45] Jang M H, Wong-Ng W, Shull R, Cook L P, Suh J S and Ko T 2003 Fabrication of long-length & bulk HTS conductors *ACerS: 105th Annual Meeting of the American Ceramic Society (Nashsville, TN, April 2003)* (*Ceramic Transactions* vol 149) ed R Meng, A Goyal and W Wong-Ng (Nashville, TN: American Ceramic Society) pp 83–93 (2004)
[46] Kang H *et al* 2001 *IEEE Trans. Appl. Supercond.* **11** 2216–9
[47] Amemiya N, Jiang ZS, Yamagishi K and Sasaoka T 2002 *IEEE Trans. Appl. Supercond.* **12** 1599
[48] Fukui S, Kitoh Y, Numata T, Tukamoto O, Fujikami J and Hayashi K 1998 *Adv. Cryog. Eng.* **44** 723
[49] Ashworth S P, Ciszek M, Campbell A M, Liang Y W and Glowacki B A 1996 *Chin. J. Phys.* **34** 232–42
[50] Ciszek M, Ashworth S P, Campbell A K, Garre R and Conti S 1998 *Supercond. Sci. Technol.* **9** 379–84
[51] Grow A, Joo J, Sighn J P, Poeppel R B and Warsynski T 1994 *Appl. Supercond.* **2** 401–10